# NEW IDEAS IN THE THEORY OF EXTRASOLAR GIANT PLANETS AND BROWN DWARFS

ADAM BURROWS, BILL HUBBARD, and JONATHAN LUNINE University of Arizona

MARK MARLEY

New Mexico State University

and

DIDIER SAUMON Vanderbilt University

#### I. INTRODUCTION

The study of extrasolar giant planets (EGPs<sup>\*</sup>) and brown dwarfs via reflex stellar motion, broad-band photometry, and spectroscopy has finally come into its own. Doppler spectroscopy alone has revealed about 15 objects in the giant planet/brown dwarf regime, including companions to  $\tau$  Boo, 51 Peg, v And, 55 Cnc,  $\rho$  CrB, 70 Vir, 16 Cyg B, and 47 UMa (Noyes et al. 1997; Butler et al. 1997; Cochran et al. 1997; Marcy & Butler 1996; Butler & Marcy 1996; Mayor & Queloz 1995; Latham et al. 1989).

The direct detection of Gl229 B (Oppenheimer et al. 1995; Nakajima et al. 1995; Matthews et al. 1996; Geballe et al. 1996; Marley et al. 1996; Allard et al. 1996; Tsuji et al. 1996) was a milestone since Gl229 B displays methane spectral features and low surface fluxes that are unique to objects with effective temperatures (in this case,  $T_{\rm eff} \sim 950$ K) below those at the solar-metallicity main sequence edge (~1750 K, Burrows et al. 1993). In addition, the almost complete absence of spectral signatures of metal oxides and hydrides (such as TiO, VO, FeH, and CaH) is in keeping with theoretical predictions that these species are depleted in the atmospheres of all but the youngest (hence, hottest) substellar objects and are sequestered in condensed form below the photosphere (Lunine et al. 1989; Marley et al. 1996). The wide range in mass and period, as well as the proximity of many of the

[1]

<sup>\*</sup> We use this shorthand for <u>Extrasolar Giant Planet</u>, but the terms "exoplanet" or "super-jupiter" are equally appropriate.

planets/brown dwarfs to their primaries, was not anticipated by most planetary scientists. Though the technique of Doppler spectroscopy used to find these companions selects for massive, nearby objects, their variety and existence is a challenge to conventional theory. Since direct detection is now feasible, and has been demonstrated by the recent acquisition of Gl229 B, it is crucial for the future of extrasolar giant planet searches that the spectra, colors, evolution, and physical structure of objects from Saturn's mass (0.3  $M_{\rm J}$ ) to 70  $M_{\rm J}$  be theoretically investigated.

# II. EARLY CALCULATIONS OF THE EVOLUTION AND STRUCTURE OF EXTRASOLAR GIANT PLANETS

# A. Gray Models

EGPs radiate in the optical by reflection and in the infrared by the thermal emission of both absorbed stellar light and the planet's own internal energy. In Burrows et al. (1995) and Saumon et al. (1996), the EGPs were assumed to be fully convective at all times. We included the effects of "insolation" by a central star of mass  $M_*$  and considered semi-major axes (a) between 2.5 A.U. and 20 A.U. Giant planets may form preferentially near 5 A.U. (Boss 1995), but as the new data dramatically affirm, a broad range of semi-major axes can not be excluded. In these calculations, we assumed that the Bond albedo of an EGP is that of Jupiter (~0.35). For the Burrows et al. (1995) study, we evolved EGPs with masses from 0.3  $M_{\rm J}$  (the mass of Saturn) through 15  $M_{\rm J}$ . Whether a 15  $M_{\rm J}$  object is a planet or a brown dwarf is largely a semantic issue, though one might distinguish gas giants and brown dwarfs by their mode of formation (e.g., in a disk or "directly").

If 51 Peg b is a gas giant, its radius is only  $1.2 \text{ R}_{\text{J}}$  and its luminosity is about  $3.5 \times 10^{-5} L_{\odot}$ . This bolometric luminosity is more than  $1.5 \times 10^4$  times the present luminosity of Jupiter and only a factor of two below that at the edge of the main sequence. The radiative region encompasses the outer 0.03% in mass, and 3.5% in radius. The study by Guillot et al. (1996) demonstrated that 51 Peg b is well within its Roche lobe and is not experiencing significant photoevaporation. Its deep potential well ensures that, even so close to its parent, 51 Peg b is **stable**. If 51 Peg b were formed beyond 1 A.U. and moved inward on a timescale greater than ~  $10^8$  years, it would closely follow a  $R_p \sim$  $R_J$  trajectory to its equilibrium position.

#### **B.** Non–Gray Models

However, to credibly estimate the infrared band fluxes and improve upon the black body assumption made in Burrows et al. (1995) and

Saumon et al. (1996), we have recently performed **non-gray** simulations at solar-metallicity of the evolution, spectra, and colors of isolated EGP/brown dwarfs down to T<sub>eff</sub>s of 100 K (Burrows et al. 1997). Figure 1 portrays the luminosity versus time for objects from Saturn's mass  $(0.3 \ M_{\rm J})$  to  $0.2 \ M_{\odot}$  for this model suite. The early plateaux between  $10^6$  years and  $10^8$  years are due to deuterium burning, where the initial deuterium mass fraction was taken to be  $2 \times 10^{-5}$ . Deuterium burning occurs earlier, is quicker, and is at higher luminosity for the more massive models, but can take as long as  $10^8$  years for a 15  $M_{\rm I}$  object. The mass below which less than 50% of the "primordial" deuterium is burnt is  $\sim 13 M_{\rm J}$  (Burrows et al. 1995). On this figure, we have arbitrarily classed as "planets" those objects that do not burn deuterium and as "brown dwarfs" those that do burn deuterium, but not light hydrogen. While this distinction is physically motivated, we do not advocate abandoning the definition based on origin. Nevertheless, the separation into M dwarfs, "brown dwarfs", and giant "planets" is useful for parsing by eye the information in the figure.

In Fig. 1, the bumps between  $10^{-4} L_{\odot}$  and  $10^{-3} L_{\odot}$  and between  $10^8$  and  $10^9$  years, seen on the cooling curves of objects from  $0.03 M_{\odot}$  to  $0.08 M_{\odot}$ , are due to silicate and iron grain formation. These effects, first pointed out by Lunine et al. (1989), occur for T<sub>eff</sub>s between 2500 K and 1300 K. The presence of grains affects the precise mass and luminosity at the edge of the main sequence. Since grain and cloud models are problematic, there still remains much to learn concerning their role and how to model them (Lunine et al. 1989; Allard et al. 1997; Tsuji et al. 1996).

# **III. NEW INSIGHTS**

The studies of Burrows et al. (1997) and Marley et al. (1996) reveal major new aspects of EGP/brown dwarf atmospheres that bear listing and that uniquely characterize them. Below  $T_{eff}$ s of 1300 K, the dominant equilibrium carbon molecule is  $CH_4$ , not CO, and below 600 K the dominant nitrogen molecule is  $NH_3$ , not  $N_2$  (Fegley & Lodders 1996). In objects with  $T_{eff} \leq 1300$  K, the major opacity sources are  $H_2$ ,  $H_2O$ ,  $CH_4$ , and  $NH_3$ . For  $T_{effs}$  below  $\sim 400$  K, water clouds form at or above the photosphere (defined where  $T = T_{eff}$ ) and for  $T_{effs}$  below 200 K, ammonia clouds form (viz., Jupiter). Collision-induced absorption of H<sub>2</sub> partially suppresses emissions longward of  $\sim 10 \ \mu m$ . The holes in the opacity spectrum of  $H_2O$  that define the classic telluric IR bands also regulate much of the emission from EGP/brown dwarfs in the near infrared. Importantly, the windows in  $H_2O$  and the suppression by  $H_2$ conspire to force flux to the blue for a given  $T_{eff}$ . The upshot is an exotic spectrum enhanced relative to the black body value in the Jand H bands (~1.2  $\mu$ m and ~1.6  $\mu$ m, respectively) by as much as two

to ten orders of magnitude, depending upon  $T_{eff}$ . The enhancement at 5  $\mu$ m for a 1 Gyr old, 1  $M_{\rm J}$  extrasolar planet is by four orders of magnitude. As  $T_{eff}$  decreases below ~1000 K, the flux in the M band  $(\sim 5 \ \mu m)$  is progressively enhanced relative to the black body value. While at 1000 K there is no enhancement, at 200 K it is near  $10^5$ . The J, H, and M bands are the premier bands in which to search for cold substellar objects. The Z band (~1.05  $\mu$ m) is also in excess of the black body value over this  $T_{eff}$  range. Even though K band (~2.2  $\mu$ m) fluxes are generally higher than black body values, H<sub>2</sub> and CH<sub>4</sub> absorption features in the K band decrease its importance relative to J and H. As a consequence of the increase of atmospheric pressure with decreasing  $T_{eff}$ , the anomalously blue J - K and H - K colors get bluer, not redder. The K and J versus J - K infrared H-R diagrams loop back to the blue below the edge of the main sequence and are not continuations of the M dwarf sequence into the red. The difference between the black body curves and the model curves is between 3 and 10 magnitudes for J versus J - K, more for K versus J - K. Gl229 B fits nicely among these theoretical isochrones. The suppression of K by  $H_2$  and  $CH_4$  features is largely responsible for this anomalous blueward trend with decreasing mass and  $T_{eff}$ .

# IV. ATMOSPHERIC COMPOSITIONS OF EGPS, CON-DENSATION, AND CLOUDS

The molecular compositions of the exotic, low-ionization atmospheres of EGPs and brown dwarfs can serve as diagnostics of temperature, mass, and elemental abundance and can help define a spectral sequence, just as the presence or absence of spectral features associated with various ionization states of dominant, or spectroscopically active, atoms and simple molecules does for M through O stars. However, the multiplicity of molecules that appear in their atmospheres lends an additional complexity to the study of substellar mass objects that is both helpfully diagnostic and confusing. Nowhere is the latter more apparent than in the appearance at low temperatures of refractory grains and clouds. These condensed species can contribute significant opacity and can alter an atmosphere's temperature/pressure profile and its albedo. Grain and cloud droplet opacities depend upon the particle size and shape distribution and these are intertwined with the meteorology (convection) in complex ways. Furthermore, condensed species can rain out and deplete the upper atmosphere of heavy elements, thereby changing the composition and the observed spectrum. In brown dwarf and EGP atmospheres, abundance and temperature/pressure profiles, particle properties, spectra, and meteorology are inextricably linked.

The formation of refractory silicate grains below 2500 K was already shown by Lunine et al. (1989) and Burrows et al. (1989) to influence the evolution of late M dwarfs and young brown dwarfs through their "Mie" opacity. The blanketing effect they provide lowers the effective temperature (T<sub>eff</sub>) and luminosity (L) of the main sequence edge mass from about 2000 K and  $10^{-4} L_{\odot}$  to about 1750 K and  $6 \times 10^{-5} L_{\odot}$ , an effect recently verified by Chabrier et al. (1998). In addition, grain opacity slightly delays the cooling of older brown dwarfs, imprinting a slight bump on their luminosity/age trajectories (see Fig. 1). The presence of grains in late M dwarf spectra was invoked to explain the weakening of the TiO bands and the shallowing of their H<sub>2</sub>O troughs in the near infrared (Tsuji et al. 1996; Jones & Tsuji 1997). Tsuji and collaborators concluded that titanium was being depleted into refractories, a conclusion with which we agree.

With a  $\rm T_{eff}$  of  ${\sim}950$  K, a luminosity below  $10^{-5}~L_{\odot}\,,$  and spectra or photometry from the R band through 5  $\mu$ m, Gl229 B hints at or exemplifies all of the unique characteristics of the family: metal (Fe, Ti, V, Ca, Mg, Al, Si) depletions, the dominance of  $H_2O$  vapor, the appearance of CH<sub>4</sub> and alkali metals, and the signatures of clouds. Clouds of low-temperature condensible species above the photosphere are the most natural explanation for the steep drop below 1  $\mu$ m in the Keck spectra between 0.83  $\mu$ m and 1  $\mu$ m (Oppenheimer et al. 1998). These clouds might not be made up of the classic silicate refractories formed at much higher temperatures, since these species may have rained out. From simple Mie theory, their mean particle size must be small (~ 0.1  $\mu$ m) in order to influence the "optical" without much perturbing the near infrared. In addition, such a population of small droplets can help explain why Gl229 B's near-infrared troughs at 1.8  $\mu m$  and 3.0  $\mu m$  are not as deep as theory would otherwise have predicted. Just as Tsuji and collaborators have shown that silicate grains at higher temperatures can shallow out the  $H_2O$  troughs, so to can species that condense at lower temperatures ( $\leq 1000 \text{ K}$ ?) explain the shallower-than-predicted Gl229 B H<sub>2</sub>O troughs. What those species might be can be illuminated by chemical abundance studies (Burrows & Sharp 1998). Note that a cloud grammage in these small-radius, lowtemperature refractories of only  $\sim 10^{-5}$  gm cm<sup>-2</sup> would be adequate to explain the anomalies.

#### A. Abundance and Condensate Results

At temperatures of ~1500–2000 K, the standard refractories, such as the silicates, spinel, and iron, condense out into grain clouds which by their large opacity lower the  $T_{\rm eff}$  and luminosity of the main sequence edge (Burrows et al. 1993; Burrows & Sharp 1998) and alter in detectable ways the spectra of objects around the transition mass (Jones & Tsuji 1997). As  $T_{\rm eff}$  decreases below that at the stellar edge, the classical refractories are buried progressively deeper below the photosphere and less refractory condensates and gas–phase molecules come to dominate (Marley et al. 1996; Burrows et al. 1997).

Below temperatures of ~1500 K, the calculations of Burrows & Sharp (1998) demonstrate and confirm that the alkali metals, which are not as refractory as Fe, Al, Ca, Ti, V, and Mg, emerge as important atmospheric and spectral constituents. At still lower temperatures, chlorides and sulfides appear, some of which will condense in the cooler upper atmosphere and form clouds that will affect emergent spectra and albedos. Cloud decks of many different compositions at many different temperature levels are expected, depending upon  $T_{\rm eff}$  (and weakly upon gravity). Clouds of chlorides and sulfides at temperature levels below ~1000 K may be responsible for the steeper slope observed in the spectrum of Gl229 B at the shorter wavelengths (Oppenheimer et al. 1998). At slightly higher temperatures, MnS, ZnS, NaAlSi<sub>3</sub>O<sub>8</sub>, KAlSi<sub>3</sub>O<sub>8</sub>, V<sub>2</sub>O<sub>3</sub>, and MgTi<sub>2</sub>O<sub>5</sub> may play a role, but only if their constituents are not scavenged into more refractory compounds and rained out deeper down.

As T<sub>eff</sub> decreases (either as a given mass cools or, for a given age, as we study objects with lower masses), the major atmospheric constituents of brown dwarfs and EGPs change. This change is reflected in which spectral features are most prominent and in the albedos of substellar objects near their primaries. Equilibrium chemical sequences are predominantly a function of temperature and can help to define a spectral sequence for substellar objects from the main sequence edge near 2000 K to EGPs with  $T_{effs}$  of a few hundred Kelvin. The appearance and disappearance of various molecules and refractories delineates an effective temperature sequence and the new proposed "L" dwarf spectral classification (Kirkpatrick et al. 1998) may correspond to a subset of such a compositional sequence. Very crudely, the "L" spectral type suggested by Kirkpatrick et al. (1998) would correspond to  $T_{\rm eff}s$  between about  $\sim 1500$  K and  $\sim 2200$  K. All but the youngest and most massive brown dwarfs and only the very youngest EGPs could have this proposed spectral designation. Most brown dwarfs and EGPs will be of an even later spectral type, yet to be coined, a spectral type that would include Gl229 B.

# B. Clouds

Cloud formation refers to the production of solid or liquid particles in the atmosphere of a brown dwarf or extrasolar planet. Cloud formation in the Earth's troposphere is a complex phenomenon involving a single species (water), two phases, multiple particle size distributions, incompletely–known particle properties and myriad cloud morphologies. The range of radiative properties of terrestrial clouds is commensurately broad, and different types of clouds can serve to either warm or cool the surface of the Earth. Much of the complexity lies in the heterogeneous distribution of such clouds in vertical and horizontal directions; the problem of treatment of the radiative transfer of broken clouds remains a difficult one (Goody & Yung 1989). Furthermore, cloud formation itself contributes latent heat to an atmosphere and, hence, can destabilize a radiative region, requiring treatment of the heat transfer by moist convection (Emanuel 1994). Cloud-forming species are known or suspected to be present in eight of the nine planets of the solar system, as well as two of the moons of the outer solar system (Titan and Triton).

The giant planets of our solar system remain the best guide to the study of clouds in brown dwarfs and extrasolar giant planets, because the background gas is hydrogen-helium in all cases, and the atmospheres are not thin layers atop a solid surface. Principal cloud forming species in the upper Jovian and Saturnian atmosphere are ammonia. water, and possibly ammonium hydrosulfide; in Uranus and Neptune they are methane and either ammonium hydrosulfide or hydrogen sulfide (Baines et al. 1995). However, a number of minor species may participate in cloud formation, and stratospheric photochemical hazes are generated by the action of solar ultraviolet radiation. In situ observations of Jupiter's cloud structure by the Galileo entry probe revealed the extent of heterogeneity across the surface of a gas giant planet; the probe failed to detect anything but very a tenuous and narrow cloud layer (Ragent et al. 1995). Since ample visual and spectroscopic evidence exist for widespread clouds on Jupiter (Carlson et al. 1995), the Galileo probe must have found a region of unusual dryness. This notion is supported by the observation that the probe fell into a "hot spot," a region of unusually high 5-micron emission (Orton et al. 1996).

Modeling a potentially broad range of compositions and properties from the small number of detailed observations of clouds available to date is daunting. One strategy is to consider end-member cloud models, characterized by simple condensation in a radiative atmosphere on the one hand, and by large scale vertical motions driven by thermal convection or other processes on the other (Lunine et al. 1986; 1989). Such models can be reduced to a few parameters which can then be constrained, albeit weakly, with spectral observations of the atmosphere. In the radiative case the cloud mass density versus altitude is determined by the saturation vapor pressure and an assumed value for the meteorological supersaturation, which determines the condensable available to form clouds, but is determined for the Earth empirically (Emanuel 1994). This factor is difficult to determine a priori for an object in which the clouds cannot be directly studied, but can be crudely estimated (Rossow 1978). A simple prescription for the cloud number density for a convectively unstable brown dwarf atmosphere is given by Lunine et al. (1989). In each case the mean particle size can be determined semi-analytically (Rossow 1978) or by use of a numerical particle growth model (Yair et al. 1995). The problem with the former approach is that the mean particle size can be significantly underestimated, based on terrestrial experience, and a size distribution is not obtained. The numerical approach suffers from the problem of poor specificity of input parameters when applied to extrasolar planets and brown dwarfs.

Spectroscopy of Gliese 229 B suggests that grain formation may be occurring in its atmosphere. Grains both alter the spectral contrast of molecular lines and, through condensation, remove gas phase species that may be directly responsible for various absorption features. Because of condensation, silicate or iron features in the spectrum may disappear at around or above 1000 K, with gaseous water bands doing the same around 400 K. The effects of clouds on the albedo or reflectivity of a brown dwarf or extrasolar planet are also large. Modeling by Marley et al. (1998) suggests large variations (factors of two or more) in the albedo of a brown dwarf or extrasolar planet, depending upon the type of cloud (large–particle convective versus small-particle laminar clouds). The four giant planets all have surface reflectivities influenced by a combination of cloud and gas opacity sources, to varying extents.

Further progress in quantifying the extent of the effects of clouds on brown dwarf atmospheres will require more realistic models of cloud formation, transport and growth of particles, data on indices of refraction of cloud particles, and incorporation of moist convective instability into radiative–convective models. These models will require additional computational resources beyond the already substantial speed and memory requirements of fully non-gray radiative-convective codes. Perhaps most challenging from a mathematical point of view is to characterize and incorporate the size-frequency spectrum of broken clouds. The problem is somewhat akin to the classical one of computing Rosseland mean absorption coefficients in grav atmosphere models, where the greatest flux contribution comes from the frequency windows of smallest opacity. Quantifying a broken cloud atmosphere through a single number characterizing percentage of area covered by clouds is likely to be highly inaccurate, because the amount of thermal radiation escaping will be highly sensitive to the gaps between the clouds. In the near-term, the most promising observations for constraining such a complex situation will be high spectral resolution data obtaining from large telescopes with sensitive electronic detectors. However, the theoretical challenge of accurately modeling broken clouds with existing computational resources remains unsolved.

#### V. MODELS OF THE BROWN DWARF GLIESE 229 B

The wide gap between stars and brown dwarfs near the edge of the main sequence on the one hand, and Jupiter on the other hand, is fortuitously occupied by the cool brown dwarf, Gl 229 B. It is sufficiently bright to allow high resolution and high signal-to-noise spectroscopy. This fascinating object displays phenomena common to giant planets and to very-low-mass stars and represents a benchmark for modeling atmospheres of EGPs. Model spectra for Gl229 B (Marley et al. 1996; Allard et al. 1996; Tsuji et al. 1996) reproduce the overall energy distribution fairly well and all agree that 1) T<sub>eff</sub> ~ 950 K, 2) the silicate opacity is small compared to the gaseous molecular opacity and can be ignored in a first approximation, and 3) the gravity of Gl229 B is poorly constrained at present. The models, however, fail to reproduce the visible flux, the observed depth of the strongest molecular absorption bands, as well as the detailed structure of the observed spectrum. The calculation of better models for Gl229 B is currently limited by the inadequate knowledge of CH<sub>4</sub> opacities and a very limited understanding of the role of grain opacity in such a cool object.

Aside from possible grain absorption and scattering, the spectrum of Gl229 B is shaped entirely by absorption by H<sub>2</sub>, H<sub>2</sub>O, CH<sub>4</sub> and, in the mid-infrared, NH<sub>3</sub>. While the opacities of H<sub>2</sub> and H<sub>2</sub>O are now well understood over the entire temperature range of interest for Gl229 B (500  $\leq T \leq 2000$  K), the current databases for CH<sub>4</sub> and NH<sub>3</sub> are limited to  $T \leq 300$  K (HITRAN database, Rothman et al. 1992) and have an incomplete wavelength coverage. In the case of CH<sub>4</sub>, this incompleteness is partly remedied by complementing the line list with frequency-averaged opacity (Karkoschka 1994; Strong et al. 1993). Because CH<sub>4</sub> plays an important role in shaping the 1 to 4  $\mu$ m spectrum of Gl229 B, the near-infrared fluxes of the present models are of limited accuracy, precisely where Gl229 B is brighter and most easily observable (Z, J, H, and K bands).

The models of Allard et al. (1996) and Tsuji et al. (1996) include TiO and VO opacities (as well as metal hydrides) which have very strong bands in the red part of the spectrum. As a consequence, their synthetic spectra reproduce the rapid decrease of the flux shortward of  $1 \mu m$ , as evidenced by R and I photometry (Matthews et al. 1996), quite nicely. However, the visible spectra of Schultz et al. (1998) and Oppenheimer et al. (1998) show a strong H<sub>2</sub>O band but *not* the bands of oxides and hydrides predicted by those models. As anticipated by Marley et al. (1996), refractory elements condense in the atmosphere of Gl229 B and are removed from the gas phase (Burrows & Sharp 1998) and a significant fraction of the condensed particles may settle to unobservable depths in the atmosphere. Fluxes from models which do not include grain opacity in the visible predict visible fluxes which are grossly in error.

The lack of any other important molecular spectral features in the visible (Griffith et al. 1998; Saumon et al. 1998) suggests that a source of continuum opacity is required. An opacity source that fits these requirements is sub-micron grains. Mie scattering theory predicts that

0.1 micron radius grains can provide substantial opacity below about 1 micron yet still be transparent at longer wavelengths (Fig. 2). In fact, such behavior is commonly observed in the solar system and has been the solution for such diverse puzzles as the radar scattering behavior of Saturn's rings particles and the spectrum of Venus' atmosphere.

Figure 2 demonstrates the dependence of the opacity of small particles upon their size. Submicron particles interact strongly with optical radiation, while affecting only slightly longer wavelengths. Griffith et al. (1998) investigated a range of possible particle optical properties and sizes and found that very red, abosorbing, submicron particles can indeed lower the optical flux of Gliese 229B, while only slightly affecting the near-infrared spectrum. Griffith et al. speculate that since Gl229 B receives twice the UV flux of Titan, an object whose atmosphere is dominated by a photochemical smog of condensates, the grains in the brown dwarf's atmosphere could also consist of photochemically– derived non–equilibrium species. Such carbonaceous material is seen throughout the solar system and is generally recognizeable by its very red color.

# A. Gravity

It is highly desirable to constrain the value of the surface gravity of Gl229 B to an astrophysically useful range. As reported by Allard et al. (1996), the spectral energy distribution of Gl229 B models is fairly sensitive to the gravity. The most gravity-sensitive colors are H - Kand J - H with  $\Delta(H - K)/\Delta(\log g) = -0.39$  and  $\Delta(J - K)/\Delta(\log g) =$ -0.26, respectively. However, the uncertainties in the photometry of Matthews et al. (1996) in these color indices are comparable to this gravity sensitivity. The present uncertainties in CH<sub>4</sub> opacities and in the role of grains also limit the ability of the models to predict reliable near-infrared colors.

Nevertheless, it is possible to constrain the gravity by analyzing the spectrum in the  $1.9 - 2.1 \,\mu$ m region (Saumon et al. 1998). In this unique part of the spectrum of Gl229 B, the absorption is completely dominated by two well-understood opacity sources: H<sub>2</sub>O and the collision-induced absorption by H<sub>2</sub>. Methane absorption is more than two orders of magnitude weaker and unlikely to become significant even when high-temperature CH<sub>4</sub> opacities become available. The importance of H<sub>2</sub>O opacity in this region is confirmed by the remarkable correspondance of the features of the observed spectrum and of the opacity of water (Geballe et al. 1996). The detailed features of the synthetic spectrum are therefore far more reliable in the  $1.9 - 2.1 \,\mu$ m region than in any other part of the spectrum. Figure 3 shows how the gravity affects the modeled features of water in this narrow spectral range. The models shown all have the bolometric luminosity of Gl229 B given by Matthews et al. 1996. The top curve shows the T<sub>eff</sub> = 870 K, log g = 4.5 model. To emphasize the effects of changing the gravity, the flux *ratio* between this model and the T<sub>eff</sub> = 940 K, log g = 5 model (middle curve) and the T<sub>eff</sub> = 1030 K, log g = 5.5) model (lower curve) are shown. If there were no gravity sensitivity, the two lower curves would be flat. This region contains thousands of H<sub>2</sub>O features and their number and depth increases with the spectral resolution. Correspondingly, the gravity sensitivity washes out at low resolution. High signal-to-noise spectroscopy at a resolution of  $R \gtrsim 1500$  should show this effect very well and has the potential of reducing the uncertainty in the surface gravity of Gl229 B to  $\pm 0.25$  dex.

#### B. Metallicity

The metallicity of late M dwarfs is notoriously difficult to determine and modern efforts are still limited to a small number of stars (see, for example, Leggett et al. 1996, Schweitzer et al. 1996, Viti et al. 1997). The metallicity of the primary star, Gl229 A, appears to be approximately solar, but is rather uncertain. Published values give [Fe/H] = -0.2 (Schiavon, Barbuy, & Singh 1997) and [M/H]=0.2(Mould 1978). The case of Gl229 B is even more problematic. The relative success of the current models indicate that Gl229 B is also approximately solar in composition. However, if the brown dwarf formed from a dissipative accretion disk, it may be analogous to the giant planets of the solar system and be enriched in heavy elements. On the other hand, phase separations in the interior may deplete the atmosphere of its heaviest elements.

Grain formation complicates the definition of the metallicity of an atmosphere. Elements are selectively removed from the gas phase and introduced in condensed phases whose composition is far more difficult to establish by spectroscopy than that of the gas. Since the gas-phase abundance of refractory elements is quite sensitive to the physics of condensation, it is best to focus on the abundant metals C, N, and O which are not significantly depleted by condensed phases in the atmosphere of Gl229 B.

The limitations of the CH<sub>4</sub> opacity database currently prevents a reliable determination of [C/H] in Gl229 B. While the opacity of H<sub>2</sub>O, the main oxygen-bearing molecule, is now well understood, the metallicity dependence of the synthetic spectra is muddled by the presence of dust affecting the near infrared. The need to untangle the veiling due to dust and the effects of metallicity on the H<sub>2</sub>O absorption bands make it very difficult to determine the [O/H] ratio in Gl229 B, although Griffith et al. (1998) find that a best fit to the optical spectrum of Gl229 B is achieved with a subsolar oxygen abundance ([O/H] = -0.2).

Our model spectra predict a strong feature of NH<sub>3</sub> near  $10.5 \,\mu\text{m}$  which has not yet been detected by observers (Marley et al. 1996, Saumon et al. 1998). The identification of NH<sub>3</sub> in the spectrum of

Gl229 B would represent the first detection of this molecule in a compact object outside of the solar system. It also offers a good possibility of measuring the [N/H] ratio, since dust opacity is negligible in Gl229 B at this long wavelength.

The model atmospheres of Burrows et al. (1997) all assumed a solar abundance of the elements. In fact, the metallicity of the sun is somewhat higher than that of the average star and it is appropriate to consider a greater variety of atmospheric metallicities. We have begun this process by computing atmosphere models for brown dwarfs in the mass and temperature range of Gliese 229 B. These exploratory models were constructed by varying the mixing ratio of all molecules uniformly away from that predicted for a solar mixture of the elements in thermochemical equilibrium. In actuality, the relative mixing ratios of the molecules will not change uniformly as the overall metallicity changes. However, such departures will be slight compared to the large range in overall metallicity that we have considered.

Low-resolution spectra for three models, each with  $T_{eff} = 1000 \,\mathrm{K}$ and  $g = 1000 \,\mathrm{m \, sec^{-2}}$ , but with varying metallicities, are presented in Fig. 4. The models were computed following the procedures in Burrows et al. (1997), although the treatment of Rayleigh scattering has been improved. In the figure, the metallicities are varied over the exceptionally large range of [Fe/H] = -2 to 1 to demonstrate the overall trends. Generally, as the metallicity decreases, the temperature profile adjusts. More flux emerges in the 3 to  $5\,\mu m$  band as the continuum molecular opacity falls. Surprisingly, this redistribution of flux results in a decrease in the flux emerging from the depths of the near-infrared water bands. Instead, the lower molecular opacity in the window regions allows more flux to emerge from deeper, hotter layers of the atmosphere resulting in a larger flux in the windows, a cooler upper atmosphere, and less flux in the depths of the near-infrared water and methane bands. Beyond about  $2\,\mu\text{m}$ , the overall flux rises as the metallicity increases. The larger metallicity closes off the near-infrared windows, raising the upper atmosphere temperature, and increasing the continuum flux.

The changes in metallicity considered above produce relatively few changes in the color differences of Gl229 B-like models, particularly for solar and subsolar abundances. Significant changes are found only for increases in metallicity above solar. J - H and J - K are most sensitive to such metallicity variations, as both colors become redder as the metallicity increases above solar. H - K and K - L' are relatively insensitive.

#### C. Convection

The molecules found in the atmosphere of a brown dwarf or EGP constrain atmospheric structure, dynamics, and chemistry. By identifying the atmospheric composition, spectroscopy provides information on the physical processes which govern the atmosphere.

Departures of atmospheric composition from equilibrium are especially interesting. CO, PH<sub>3</sub>, GeH<sub>4</sub>, and AsH<sub>3</sub> have all been detected in Jupiter's atmosphere at abundances many orders of magnitude higher than expected from equilibrium chemistry (see review by Fegley & Lodders 1994). The presence of these non-equilibrium molecules is taken to be evidence of convection. Since convective timescales are shorter than chemical equilibrium timescales, these molecules can be dredged up from deeper in Jupiter's interior and transported to the visible atmosphere.

In Gl229 B, the detection of CO in abundances in excess of that predicted for chemical equilibrium (Noll et al. 1997) implies that the visible atmosphere (near 800 to 1400 K) must also be convective. Yet many atmosphere models find that the radiative-convective boundary lies far deeper, below 1700 K. However, the models of Marley et al. (1996) and Burrows et al. (1997) predict an additional, detached, upper convection zone. Such a zone would transport CO to the visible atmosphere from depths where it is more abundant. Other molecules may also trace convection, including PH<sub>3</sub>. The chemical equilibrium profile of Cs is very similar to that of CO (Burrows & Sharp 1998). Thus, the same convection that dredges CO must also be dredging Cs. However, the lack of TiO and other refractory diatomics in the spectrum suggest that the atmosphere is not fully convective to the depth (below 2000) K) where these molecules condense. Taken together, these results may support the presence of a detached convection zone. Thus, CO and Cs may be tracing the vertical convective structure of the brown dwarf. A similar radiative zone, lying below Jupiter's visible turbulent atmosphere, has been predicted by Guillot et al. (1994). A confirmation of such a zone at Gl229 B would strengthen the argument for such a zone in Jupiter. PH<sub>3</sub> is also potentially detectable in Gl229 B by spacebased platforms and will also act as a tracer of convection (Noll et al. 1997). Measurements of the abundances of this suite of molecules in a variety of objects may map out the atmospheric dynamics of substellar objects.

Photochemistry driven by incident radiation can also produce important non-equilibrium species. Thus, many hydrocarbons are found in the atmospheres of the solar Jovian planets, including  $C_2H_2$  and  $C_2H_6$  that would not otherwise be expected. A rich variety of photochemical products will likely be found in the atmospheres of the extrasolar planets, particularly those with warm atmospheres and large incident fluxes. Hazes produced by the condensation of some species can produce signatures in the spectra of these objects far in excess of what might be expected given their small mixing ratios.

# VI. ALBEDOS AND THE REFLECTIVITY OF EGPS

Both scattered light from the primary star and thermal emission by a planet contribute to a planet's spectrum. These two components can be crudely modeled as the sum of the reflection of a high temperature Planck function characterizing light from the primary plus a second, lower temperature, Planck function representing the thermal emission from the planet itself (Saumon et al. 1996). For the planets of our solar system, the two Planck functions are well separated in wavelength. This can be seen from the Wien displacement law,  $\lambda T = 0.29$  cm deg. For a 6000 K primary and a planet radiating at 200 K, the Planck functions of the primary and planet peak at 0.48  $\mu$ m and 14.5  $\mu$ m respectively. This separation in the bulk of the radiation field from the planets and the Sun has led to a specialized nomenclature in which "solar" and "planetary" radiation are often treated separately.

However, for an arbitrary planet orbiting at an arbitrary distance from its primary, there can be substantial overlap of the two Planck functions. A general theory of extrasolar atmospheres must consistently compute the absorbed and scattered incident light. Marley (1998) has generated exploratory EGP atmosphere models that include deposition of incident radiation. He finds that in typical EGP atmospheres absorption in the strong near–IR water and methane bands produces temperature inversions above the tropopause, similar to Jupiter's stratosphere. Generation of a comprehensive suite of model reflected and emitted spectra will require that a large range of primary stellar types, orbital distances, and planetary masses and ages be investigated.

Planets are brightest near the peak in the solar Planck function and the reflected flux falls off at shorter and longer wavelengths. To remove the effects of the solar spectrum and more clearly understand the processes acting in the planet's atmosphere, the reflected spectra of planets are commonly presented as geometric albedo spectra. The geometric albedo is essentially the planetary spectrum divided by the solar spectrum. Formally, it is the ratio of the flux received at Earth at opposition to the flux that would be received by a Lambert disk of the same size as the planet at its distance from the sun.

Reflected planetary spectra can also be approximated by computing wavelength-dependent geometric albedos of EGP atmospheres. The resultant planetary spectrum is then the sum of the emitted flux plus the product of the incident radiation times the geometric albedo with a phase correction. Figure 5 compares the geometric albedo spectra of Jupiter and Uranus. A purely Rayleigh scattering planet would have a geometric albedo of 0.75 at all wavelengths.

As Fig. 5 demonstrates, planets are not gray reflectors. They reflect best near  $0.5 \,\mu\text{m}$  where Rayleigh scattering dominates the reflected flux. At shorter wavelengths, Raman scattering, which shifts some UV photons to longer wavelengths, and absorption by the ubiqui-

to us high altitude haze found throughout the outer solar system, lower the geometric albedo. Longward of  $0.6\,\mu{\rm m}$  the strength of molecular rotational-vibrational bands increases and molecular absorption, rather than scattering, begins to dominate the spectrum. Methane and the pressure-induced bands of hydrogen are the most important absorbers. In between the molecular bands, solar photons reach bright cloud decks and are scattered. So the planets remain bright in some band passes.

Marley et al. (1998) computed geometric albedo spectra for a large variety of EGPs, ranging from planets of less than 1 Jupiter mass to the most massive brown dwarfs. They considered objects with effective temperatures between 100 and 1200 K and found that the UV and optical spectra of extrasolar giant planets are generally similar to those of the solar giant planets. At longer wavelengths, however, the reflected flux depends critically on the presence or absence of atmospheric condensates. When condensates are present, photons have the opportunity to scatter before they are absorbed.

The most important condensate in EGP atmospheres is water. Water clouds appear as EGPs cool through effective temperatures of about 400 K. The sudden appearance of water clouds brightens the planets in reflected red and IR light, as shown in Figure 6. This figure presents a computed spectrum for an extrasolar planet orbiting at 1 A.U. from a G2V primary. Also shown is the emitted flux for an object with  $T_{\rm eff} = 400$  K. It is apparent from this plot that the thermal emission dominates in the infrared for cloud-free objects. However, once clouds form they will both attenuate the emitted flux and reflect a far larger proportion of the incident radiation. Of course, there will be a continuum such that for objects with the same effective temperature, but which are closer to their primary, the reflected flux will surpass the emitted flux. The emitted flux will continue to be important at lower temperatures for objects further from their primaries. Again, individual models are required for each specific case.

The ratio of the total reflected light to the total light incident upon a planetary atmosphere (Bond albedo) depends sensitively on the spectral distribution of the incident radiation. For example, most of the flux of an A star emerges in the UV and blue. When incident upon a giant planet, most of this light may be Rayleigh scattered, resulting in a large Bond albedo. In contrast, the predominantly red and infrared photons from an M star are far more likely to be absorbed. Thus, the Bond albedo of the same planet, when illuminated by two different stars, could vary by up to an order of magnitude, as the stellar type of the primary varies (Marley et al. 1998). Note that nonequilibrium photochemical hazes can darken the planets in the UV, further complicating the reflected spectra and energy budgets.

# VII. THE RELATIONSHIP BETWEEN GIANT PLANETS OF THE SOLAR SYSTEM AND EGPS

The advent of the science of EGPs and brown dwarfs, with its many new discoveries outside the solar system, should not cause us to lose sight of the central role of our local giant planets as exemplars that can be studied in unrivaled detail. There are still many questions that remain concerning Jupiter's and Saturn's formation and cooling histories that we must answer before we can confidently tackle their analogs beyond the solar system. One of the issues that still surrounds the study of our gas giants is the character, radial distribution, and origin of their compositions. Do they have a common formation mechanism with the newly discovered substellar objects, or is there a distinct mass-related boundary between the formation of such giant planets ( $\sim 0.001 M_{\odot}$ ) and brown dwarfs ( $\sim 0.01 M_{\odot}$ ) (see M. Mayor et al., this volume) that is reflected in their compositions? Jupiter and Saturn provide unique laboratories by which we can address these and related questions of fundamental interest to planetary science and astronomy.

#### A. Non–Solar Metallicities and Implications for Formation

The solar system exhibits a progressive change in the bulk composition of its four giant planets as a function of heliocentric distance. According to interior models constrained by improvements in the hydrogen-helium equation of state and by the Galileo entry probe results for the abundance of helium in the Jovian atmosphere, Jupiter is close to bulk solar composition, with a probable enhancement of C, N, and O by about a factor of  $\sim 5$ , distributed uniformly in its envelope, and with limits on a dense central core amounting to > 0.02 by mass fraction (or about 6 earth masses maximum) (Guillot, Gautier, and Hubbard, 1997). Models of Saturn, on the other hand, are distinctly nonsolar, with envelope enhancements of C, N, and O by about twice the Jovian factor, and a similar dense core of  $\sim 6$  to 8 earth masses (Guillot et al. 1994). Uranus and Neptune models seem to resemble a larger version of the Saturn or Jupiter core with a thin ( $\sim 0.1$  by mass) envelope of hydrogen and helium (Hubbard, Podolak, and Stevenson 1995).

The traditional interpretation of this sequence, which is now open to revision in the light of recent detections of extrasolar giant planets and recent downward revisions of the Jupiter and Saturn core masses, is that the giant planets Jupiter and Saturn formed by the capture of nebular hydrogen and helium onto dense Uranus/Neptune–like cores (Mizuno, Nakazawa, and Hayashi 1978), with subsequent significant accretion of icy cometesimals being responsible for enrichment of C, N, and O-bearing molecules in their envelopes. Presumably, the capture of nebular hydrogen onto proto–Uranus and proto–Neptune was less efficient owing to lower nebular density at their orbital radii and slower accretion of their dense icy cores.

The detection of EGPs at very small orbital radii has strongly suggested the possibility of significant radial migration of giant planets during the nebular phase (Trilling et al. 1998). Recent observations (Terebey et al. 1998) may support the possibility of direct formation of giant planets without the necessity of an initial dense core to trigger hydrodynamic accretion of hydrogen-helium gas.

### **B.** Constraints on Cooling Mechanisms

The luminosity of a giant planet is determined by the heat radiated into space by means of depletion of its interior entropy as determined by the atmospheric boundary condition. The latter is strongly affected by metallicity. Moreover, the heat evolved can be strongly increased by a redistribution of hydrogen (with high specific entropy) toward shallower, lower-temperature regions of the planet, while denser components (with lower specific entropy) sink to deeper, hotter regions. Thus, atmospheric depletion of metals and helium may be accompanied by higher luminosity. It is this effect which is believed to be responsible for the anomalously high luminosity of Saturn (Stevenson & Salpeter 1977).

In principle, the detection of EGPs, whose values of luminosity, age, mass, and atmospheric composition can be determined, will provide a test of this concept along with constraints on the hydrogen phase diagram. The latter predicts that helium separation may be important for objects with  $M < 0.001 M_{\odot}$ , while possible segregation of other species via a first–order phase transition in hydrogen may occur in objects with masses  $M < 0.01 M_{\odot}$ .

### ACKNOWLEDGMENTS

We thank David Sudarsky, Christopher Sharp, Richard Freedman, Shri Kulkarni, Jim Liebert, Davy Kirkpatrick, France Allard, Gilles Chabrier, Ben Oppenheimer, Chris Gelino, and Tristan Guillot for a variety of useful contributions. This work was supported under NASA grants NAG5-7499, NAG5-7073, NAG5-4988, and NAG5-2817 and under NSF grant AST93-18970.

# REFERENCES

- Allard, F., Hauschildt, P.H., Baraffe, I., & Chabrier, G. 1996. Synthetic spectra and mass determination of the brown dwarf Gl229 B. Astrophys. J. Lett. 465:L123–L127.
- Allard, F., Hauschildt, P. H., Alexander, D. R. & Starrfield, S. 1997. Model atmospheres of very low mass stars and brown dwarfs. Ann. Rev. Astron. Astrophys. 35:137–177.
- Allard, F. 1998. Model atmospheres: Brown dwarfs from the stellar perspective. In *Brown dwarfs and extrasolar planets*, ASP conference Series Vol. 134, eds. R. Rebolo, E.L. Martín and M.R. Zapatero Osorio (San Francisco: Astronomical Society of the Pacific), pp. 370–382.
- Baines, K.H., Hammel, H.B., Rages, K.A., Romani, P.N., & Samuelson, R.E. 1995. Clouds and hazes in the atmosphere of Neptune. In *Neptune and Triton*, (Ed. D.P. Cruikshank). Tucson: University of Arizona Press, pp. 489–546.
- Boss, A. 1995. Proximity of Jupiter-like planets to low-mass stars. Science 267:360–362.
- Burrows, A., Hubbard, W.B., & Lunine, J.I. 1989. Theoretical models of vow low mass stars and brown dwarfs. Astrophys. J. 345:939– 958.
- Burrows, A., Hubbard, W.B., Saumon, D., & Lunine, J.I. 1993. An expanded set of brown dwarf and very low mass star models. Astrophys. J. 406:158–171.
- Burrows, A., Saumon, D., Guillot, T., Hubbard, W.B., & Lunine, J.I. 1995. Prospects for detection of extrasolar giant planets by next generation telescopes. *Nature* 375:299–301.
- Burrows, A., Marley, M.S., Hubbard, W.B., Lunine, J.I., Guillot, T., Saumon, D., Freedman, R.S., Sudarsky, D., & Sharp, C. 1997. A nongray theory of extrasolar giant planets and brown dwarfs. *Astrophys. J.* 491:856–875.
- Burrows, A. & Sharp, C.M. 1998. Chemical equilibrium abundances in brown dwarf and extrasolar giant planet atmospheres. submitted to *Astrophys. J.*.
- Butler, R. P. & Marcy, G. W. 1996. A planet orbiting 47 Ursae Majoris. Astrophys. J. 464:L153–L156.
- Butler, R. P., Marcy, G. W., Williams, E., Hauser, H., & Shirts, P. 1997. Three new "51 pegasi-type" planets. Astrophys. J. 474:L115–L118.
- Carlson, R.W., Baines, K.H., Orton, G.S., Encrenaz, Th., Drossart,

P., Roos-Serote, M., Taylor, F.W., Irwin, P., Wier, A., Smith, S., Calcutt, S. 1997. Near-infrared spectroscopy of the atmosphere of Jupiter. *EOS* 78 supplement:F413.

- Chabrier, G. et al. 1998. to be published in the proceedings of the first Euroconference on *Stellar Clusters and Associations*, held in Los Cancajos, La Palma, Spain, May 11–15, eds. R. Rebolo, V. Sanchez–Bejar, and M.R. Zapatero-Osorio.
- Cochran, W.D., Hatzes, A.P., Butler, R.P., & Marcy, G. 1997. The discovery of a planetary companion to 16 Cygni B. Astrophys. J. 483:457–463.
- Emanuel, K.A. 1994. Atmospheric Convection. New York: Oxford University Press.
- Fegley, B. Jr. & Lodders, K. 1994. Chemical models of the deep atmospheres of Jupiter and Saturn. *Icarus* 110:117–154.
- Fegley, B. Jr. & Lodders, K. 1996. Atmospheric chemistry of the brown dwarf Gliese 229 B: Thermochemical equilibrium predictions. Astrophys. J. Lett. 472:L37–L39.
- Geballe, T.R., Kulkarni, S.R., Woodward, C.E., & Sloan, G.C. 1996. The near-infrared spectrum of the brown dwarf Gliese 229 B. Astrophys. J. Lett. 467:L101–L104.
- Goody, R.M. & Yung, Y.L. 1989 Atmospheric Radiation: Theoretical Basis New York: Oxford University Press, 519pp.
- Griffith, C.A. et al. 1998. in preparation.
- Guillot, T., Chabrier, G. Morel, P., & Gautier, D. 1994. Nonadiabatic models of Jupiter and Saturn. *Icarus* 112:354–367.
- Guillot, T. Burrows, A., Hubbard, W.B., Lunine, J.I., & Saumon, D. 1996. Giant planets at small orbital distances. Astrophys. J. Lett. 459:L35–L38.
- Guillot, T., Gautier, D., & Hubbard, W.B. 1997. NOTE: New constraints on the composition of Jupiter from galileo measurements and interior models. *Icarus* 130:534–539.
- Hubbard, W.B., Podolak, M., & Stevenson, D.J. 1995. The Interior of Neptune. In Neptune and Triton. ed. D.P. Cruikshank (Tucson: University of Arizona Press), pp. 109–138.
- Jones, H.R.A. & Tsuji, T. 1997. Spectral evidence for dust in late-type M dwarfs. Astrophys. J. 480:L39–L41.
- Karkoschka, E. 1994. Spectrophotometry of the Jovian planets and Titan at 300 to 1000 nm wavelength: The methane spectrum. *Icarus* 111:174–192.
- Kirkpatrick, J.D., Reid, I.N., Liebert, J., Cutri, R.M., Nelson, B., Beichman, C.A., Dahn, C.C., Monet, D.G., Skrutskie, M.F., & Gizis, J. 1998. in preparation.
- Latham, D. W., Mazeh, T., Stefanik, R.P., Mayor, M., & Burki, G. 1989. The unseen companion of HD114762 - A probable brown dwarf. *Nature* 339:38–40.

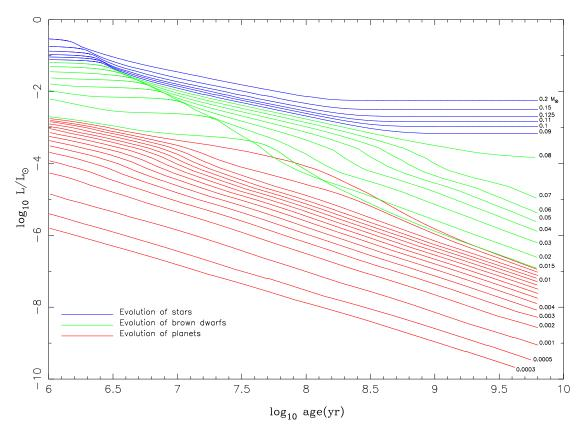
- Leggett, S.K., Allard, F., Berriman, G., Dahn, C.C., & Hauschildt, P.H. 1996. Infrared spectra of low-mass stars: Towards a temperature scale for red dwarfs. Astrophys. J. Suppl. 104:117–143.
- Lunine, J.I., Hubbard, W.B., & Marley, M. 1986. Evolution and infrared spectra of brown dwarfs. Astrophys. J. 310:238–260.
- Lunine, J.I., Hubbard, W.B., Burrows, A. S., Wang, Y.-P., & Garlow, K. 1989. The effect of gas and grain opacity on the cooling of brown dwarfs. *Astrophys. J.* 338:314-337.
- Marcy, G. W. & Butler, R. P. 1996. A planetary companion to 70 Virginis. Astrophys. J. 464:L147–L151.
- Marley, M.S., Saumon, D., Guillot, T., Freedman, R.S., Hubbard, W.B., Burrows, A., & Lunine, J.I. 1996. Atmospheric, evolutionary, and spectral models of the brown dwarf Gliese 229 B. *Science* 272:1919–1921.
- Marley, M. 1998. Atmosphers of giant planets from Neptune to Gliese 229 B. In Brown dwarfs and extrasolar planets, ASP conference Series Vol. 134, eds. R. Rebolo, E.L. Martín and M.R. Zapatero Osorio (San Francisco: Astronomical Society of the Pacific), pp. 383–393.
- Marley, M.S., Gelino, C., Stephens, D., Lunine, J.I., & Freedman, R. 1998. Reflected spectra and albedos of extrasolar giant planets I: Clear and cloudy atmospheres. submitted to Astrophys. J..
- Matthews, K., Nakajima, T., Kulkarni, S.R., & Oppenheimer, B.R. 1996. Spectral energy distribution and bolometric luminosity of the cool brown dwarf Gliese 229B. Astron. J. 112:1678–1682.
- Mayor, M. & Queloz, D. 1995. A jupiter-mass companion to a solartype star. *Nature* 378:355–357.
- Mizuno, H., Nakazawa, K, & Hayashi, C. 1978. Instability of a gaseous envelope surrounding a planetary core and formation of giant planets. *Prog. Theor. Phys* 60:699-710.
- Mould, J.R. 1978. Infrared spectroscopy of M dwarfs. Astrophys. J. 226:923–930.
- Nakajima, T., Oppenheimer, B.R., Kulkarni, S.R., Golimowski, D.A., Matthews, K., & Durrance, S.T. 1995. Discovery of a cool brown dwarf. *Nature* 378:463–465.
- Noll, K.S., Geballe, T.R., & Marley, M.S. 1997. Detection of abundant carbon monoxide in the Brown dwarf Gl229 B. Astrophys. J. Lett., 489:L87–L90.
- Noyes, R.W. et al. 1997. A planet orbiting the star Rho Coronae Borealis. Astrophys. J. Lett. 483:L111-L114.
- Oppenheimer, B.R., Kulkarni, S.R., Matthews, K., & Nakajima, T. 1995. Infrared spectrum of the cool brown dwarf Gl229 B. Science 270:1478–1479.
- Oppenheimer, B.R., Kulkarni, S.R., Matthews, K., & van Kerkwijk, M.H. 1998. The spectrum of the brown dwarf Gliese 229 B. Astro-

phys. J. 502:932–943.

- Orton, G. and 40 others. 1996. Earth-based observations of the Galileo probe entry site. *Science* 272:839–840.
- Ragent, B., Colburn, D.S., Avrin, P., Rages, K.A. 1996. Results of the Galileo Probe nephelometer experiment. *Science* 272:854–856.
- Rossow, W.B. 1978. Cloud microphysics: Analysis of the clouds of Earth, Venus, Mars and Jupiter. *Icarus* 36:1–50.
- Rothman, L.S. et al. 1992. The HITRAN molecular database Editions of 1991 and 1992. J. Quant. Spectros. Rad. Transf. 48:469– 507.
- Saumon, D., Hubbard, W.B., Burrows, A., Guillot, T., Lunine, J.I., & Chabrier, G. 1996. A theory of extrasolar giant planets. Astrophys. J. 460:993–1018.
- Saumon, D., Marley, M.S., Guillot, T., & Freedman, R.S. 1998. Spectral diagnostics for the brown dwarf Gliese 229 B, submitted to Astrophys. J..
- Schweitzer, A., Hauschildt, P.H., Allard, F., & Basri, G. 1996. Analysis of Keck high resolution spectra of VB10. Mon. Not. Roy. Astron. Soc. 283:821–829.
- Schiavon, R.P., Barbuy, B., & Singh, P.D. 1997. The FeH Wing-Ford band in spectra of M stars. Astrophys. J. 484:499–510.
- Schultz, A.B., et al. 1998. First results from the Space Telescope Imaging Spectrograph: Optical spectra of Gl229 B. Astrophys. J. Lett. 492:L181–L184.
- Stevenson, D.J. & Salpeter, E.E. 1977. The dynamics and helium distribution in hydrogen-helium fluid planets. Astrophys. J. Suppl. 35:239–261.
- Strong, K., Taylor, F.W., Calcutt, S.B., Remedios, J.J., & Ballard, J. 1993. Spectral parameters of self and hydrogen broadened methane from 2000 to 9500 cm<sup>-1</sup> for remote sounding of the atmosphere of Jupiter. J. Quant. Spectrosc. Radiat. Transfer 50:363–429.
- Terebey, S. et al. 1998. submitted to Nature.
- Trilling, D.E., Benz, W., Guillot, T., Lunine, J.I., Hubbard, W.B., & Burrows, A. 1998. Orbital evolution and migration of giant planets: modeling extrasolar planets. *Astrophys. J.* 500:428–439.
- Tsuji, T., Ohnaka, K., Aoki, W. & Nakajima, T. 1996. Evolution of dusty photospheres through red to brown dwarfs: how dust forms in very low mass objects. Astron. Astrophys. Lett. 308:L29–L32.
- Viti, S., Jones, H.R.A., Schweitzer, A., Allard. F., Hauschildt, P.H., Tennyson, J., Miller, S., & Longmore, A.J. 1997. The effective temperature and metallicity of CM Draconis. *Mon. Not. Roy. Astron. Soc.* 291:780–796.
- Yair, Y., Levin, Z., & Tzivion, S. 1995. Microphysical processes and dynamics of a Jovian thundercloud. *Icarus* 114:278–299.

# FIGURE CAPTIONS

- Figure 1. Evolution of the luminosity (in  $L_{\odot}$ ) of solar-metallicity M dwarfs and substellar objects versus time (in years) after formation (from Burrows et al. 1997). The stars, "brown dwarfs" and "planets" are shown as solid, dashed, and dot-dashed curves, respectively. In this figure, we arbitrarily designate as "brown dwarfs" those objects that burn deuterium, while we designate those that do not as "planets." The masses in  $M_{\odot}$  label most of the curves, with the lowest three corresponding to the mass of Saturn, half the mass of Jupiter, and the mass of Jupiter.
- Figure 2. Approximate Mie scattering efficiency of various-sized enstatite dust grains. Submicron grains can produce large scattering and extinction opacity at optical wavelengths and yet remain essentially invisible at longer wavelengths. However, because they scatter almost conservatively in the optical, silicates are poor candidates for the grains responsible for the lower optical flux of Gl229 B.
- Figure 3. Gravity dependence of the H<sub>2</sub>O features in the 1.9 to 2.1 micron region. The three synthetic spectra correspond to models which all have the bolometric luminosity of Gl229 B. The top curve shows the  $T_{\rm eff} = 870$  K, log g = 4.5 spectrum, used as a reference spectrum in this figure. The other curves are flux *ratios* of the  $T_{\rm eff} = 940$  K, log g = 5 spectrum to the reference spectrum, and the ratio of the  $T_{\rm eff} = 1030$  K, log g = 5.5 spectrum to the reference spectrum, shown by the middle and bottom curves, respectively. All spectra have been shifted vertically for clarity. The synthetic spectra are shown at a spectral resolution of 1500.
- Figure 4. Model thermal emission spectra for model atmospheres ( $g = 1000 \,\mathrm{m\,sec^{-2}}$ ,  $T_{\mathrm{eff}} = 1000 \,\mathrm{K}$ ) of varying metallicity. These low-resolution spectra demonstrate that broad band near–IR flux measurements will not be able to distinguish differences in metallicity below about about 1/10 solar. For larger metallicities, J band is most sensitive to increasing metallicity.
- Figure 5. Geometric albedo spectra for Uranus, Jupiter, and a model 7– Jupiter mass planet with  $T_{\rm eff} = 400$  K. The model includes no clouds, and is thus darker than either planet longward of about 0.6  $\mu$ m. Absorption by methane and water removes incident photons before they can be Rayleigh scattered in the model. In contrast, Jupiter's and Uranus' cloud decks reflect brightly in between strong methane absorption bands. Jupiter is much darker than either the model or Uranus at blue and UV wavelengths. Dark photochemical hazes are predominantly responsible for lowering the reflectivity of the planet in this spectral range.
- Figure 6. Model spectra for  $12 M_J$ ,  $T_{\rm eff} = 300 \, {\rm K}$  planet orbiting at 1 A.U. from a G2V star. Solid line shows reflected flux received at 10 pc if planet's atmosphere is cloud-free. Dotted line demonstrates enhancement in flux when water clouds are added to the model. Both models are from Marley et al. (1998). Long dashed line gives thermal emission in the case of no clouds (Burrows et al. 1997). For this object, reflected near-IR flux begins to dominate thermal emission when clouds form as the object cools through about 400 K.



 $\ensuremath{\mathsf{Evolution}}$  of luminosity with time for different masses

